Predictive Control of Sheet- and Film-Forming Processes

John C. Campbell and James B. Rawlings
Dept. of Chemical Engineering, University of Wisconsin, Madison, WI 53706

A constrained infinite-horizon model-predictive controller is advocated to improve product properties from sheet- and film-forming processes by feedback control; the proposed model structure captures the main characteristics of the process, including the scanning sensor and large time delay. Model parameters are identified from process data, and symmetry is enforced to improve the parameter estimates. The film thickness is estimated from sparse measurements using a periodic Kalman filter. The covariances of the estimates are used to evaluate scanning patterns. Integrating disturbance models are used to achieve offset free control. Detectability conditions are presented for both models to ensure that the disturbances can be estimated from the measurement. Once the state of the film is reconstructed adequately from the measurement, a control strategy can be implemented to improve film properties. One important control contribution is to enable the controller to handle hard constraints on the actuators without clipping the controller output signal. The target-tracking problem is discussed, and the uniqueness of the steady-state solution is established. By simulations an output disturbance model is compared with a measured input disturbance model.

Introduction

Of the many stages in the paper-forming process, one stage in particular determines the paper's final properties, that is, thickness, basis weight, and moisture content. This stage is the sheet-forming part of the paper process, and it involves depositing an even layer of pulp slurry onto a fourdrinier wire. In the sheet-forming part of the paper process, thick stock, consisting of treated wood fibers and water, is mixed with white liquor and pumped into a headbox. The headbox pressure is controlled to deposit a constant amount of material through a slice lip onto a moving fourdrinier wire. Some material passes down underneath the wire and is recycled as white liquor, while the rest of the material is dried and pressed to form paper (Dumont, 1986). A significant distance from the headbox, a scanning sensor measures some of the paper's properties such as thickness, basis weight, and moisture content. Manipulated variables such as actuators on the slice lip and stock flow into the headbox can be used to control the paper properties. Figure 1 shows the main features of a generic paper-making process.

Correspondence concerning this article should be addressed to J. B. Rawlings.

The extrusion process used in the production of polymer films also determines final product properties. In one stage of the film-forming process, the sheet of film is extruded through a die lip and pinned to roller conveyers. Then the film is exposed to a variety of external processes that can stretch, heat, dry, shrink, and coat the film. Further down the line, a scanning sensor measures the thickness of the film before it is rolled up on a drum as the final product (Rawlings and Chien, 1996). As with the paper-forming process, Figure 1 is an appropriate depiction of the generic film-forming process.

The paper-making and film-forming processes come from different industries, yet are structurally similar and can benefit from advanced control. Similar control problems arise also in the production of metal slabs and foils (Dumont, 1997).

Both of the preceding processes have actuators that affect final product variation. In the film process, the die is a large piece of metal that can be slightly deformed by the actuators. Limited movement of the die lip allows fine-tuning of the film thickness. In addition to the die-lip position actuator, the polymer film thickness is affected by the extruder screw

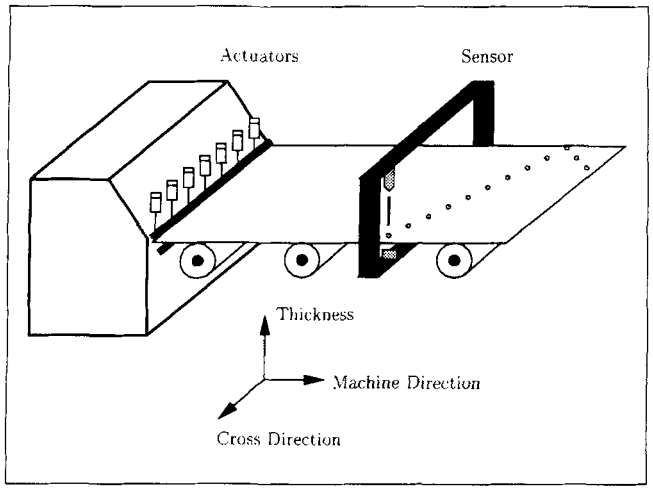

Figure 1. Film- and sheet-forming process.

speed. Control of cross-film thickness variation, rather than control of thickness itself, is the main objective of this study, and so the extruder screw speed actuator is neglected. Simultaneous control of cross and machine direction variation is addressed in Zhang (1997).

The downstream sensor consists of a radiation-emitting source and a detector. The sensor is mounted on a frame, scans back and forth over the film, and provides measurements in a zig-zag pattern along the sheet length. The sensor measurement divides the film into lanes, and only one of the lanes is measured at each time step. The sensed measurements can be used to estimate the film thickness across the sheet, and the estimate can be used in a predictive controller to remove disturbances.

It is worthwhile to point out other recent work in the area of sheet and film control. Featherstone and Braatz (1997) assume a model for a typical circular blown-film process (e.g., plastic garbage bags) and then focus on identifying the model for the purpose of control. They propose that poor performance in industrial sheet- and film-control efforts is due to model mismatch and in particular incorrect identification of the signs of the model gains. Rigopoulos et al. (1997) use principal-component analysis to determine a low-order estimation of sheet disturbances. Dave et al. (1997) use LP methods to solve large-scale sheet- and film-control problems. Kristinsson and Dumont (1996) control the parameters of orthogonal polynomials to handle the die-lip constraints, although their controller is not predictive. There has also been recent work in the area of robust control (Corscadden and Duncan, 1997; VanAntwerp et al., 1997), a topic that is not addressed in this article.

In contrast to previous work, the model parameters presented in this article are determined from plant data. The model is used in conjunction with a periodic Kalman filter to obtain optimal estimates of the film thickness (Campbell and Rawlings, 1995; Tyler and Morari, 1995). New work in the area of sheet and film estimation includes detectability conditions of the estimated disturbances and use of a measured input disturbance model to reject quickly common actuator disturbances. Finally, the constrained infinite-horizon control problem is proposed with some new insight into the statement and solution of the target-tracking problem.

Model Structure

A linear state-space model of the following form provides a starting point for modeling paper- and film-forming processes:

$$x_{k+1} = Ax_k + Bu_k$$
$$y_k = Cx_k.$$

Negligible dynamics, sparse measurements, and a large time delay are the key assumed process characteristics incorporated into the model. These characteristics are discussed by several authors, including Boyle (1977), Wilhelm and Fjeld (1983), and Rawlings and Chien (1996). Of note is the periodic measurement matrix used to handle the scanning sensor. Since the scanner reports only one measurement at every time step, a single-measurement matrix is not appropriate. C is replaced by a set of measurement matrices. These measurement matrices (row vectors for a single scanner) are denoted $\tilde{C}_j$ with j ranging from zero to $q-1$, in which q is the period of the scanning sensor. For a typical "across and back" scanning pattern the period is $2l-1$, where l is the number of lanes. Because the state is a vector of film thicknesses, a typical $\tilde{C}_j$ matrix contains zero elements except in the lane corresponding to the sensor location.

The time delay, along with fast dynamics ($A=0$) and a scanning sensor, provides the following time-varying linear model

$$x_{k+1} = Ku_{k-d}$$
$$y_k = C_k x_k, \tag{1}$$

in which $C_k = \tilde{C}_j$, $j = k \bmod q$. The notation $k \bmod q$ represents the remainder of k/q. In this model k is discrete sample time, x is a vector of film thicknesses in the cross direction, u is a vector of actuator positions, and y is the scanner measurement(s). In general, $x \in \Re^n$, where n is equal to the number of lanes; $u \in \Re^m$, where m is equal to the number of actuators; and $y \in \Re^p$, where p is equal to the number of measurements. Since many processes have a mounted scanning sensor, y is a scalar ($p=1$). The time delay, d, can be handled by enlarging the state. Either past states or past inputs can be stored. In this case, there are fewer actuators than lanes, so past inputs are stored to keep the state vector as small as possible.

Model Identification

Two parts of the model need to be determined from data. The first is the time delay, d, which is assumed constant and can be measured during routine operation. The second part of the model determined from process data is the gain matrix, K. If the steady-state assumption is valid (e.g., the film reaction to actuator movement is fast compared to the time delay), then the scanning sensor does not make the identification more difficult. Data can be obtained by injecting a unit step into an actuator and waiting for the sensor to measure all lanes. The identification problem is to determine K in the equation $Y = UK^T$, where

$$U = \begin{bmatrix} \tilde{u}_1 \\ \vdots \\ \tilde{u}_{n_e} \end{bmatrix} \in \Re^{n_e \times m} \quad \text{and} \quad Y = \begin{bmatrix} \tilde{y}_1 \\ \vdots \\ \tilde{y}_{n_e} \end{bmatrix} \in \Re^{n_e \times p}, \qquad (2)$$

$\tilde{u}_i \in \Re^{1 \times m}$ represents the positions of the m actuators during the ith experiment and $\tilde{y}_i \in \Re^{1 \times p}$ represents the thickness of the p lanes during the ith experiment (n_e total experiments). Since U may be nonsquare or may not have full rank, $Y = UK^T$ is solved for K^T using the pseudoinverse of U. In calculating the pseudoinverse, a tolerance can be chosen in order to neglect sufficiently small singular values. See Golub and Van Loan (1989) for more details on the SVD and pseudoinverse.

Identification example

The following calculation uses data from a 12-input, 12-output pilot-scale polymer film line at 3M. The third actuator was unavailable during the experiments. Four of the 36 steady-state experiments are shown in Figure 2. Absence of data relating the third actuator to the outputs generates an ill-conditioned least-squares problem. The pseudoinverse is obtained by taking the singular-value decomposition of U and inverting only the nonzero singular values. The estimated gain matrix is shown as a shaded picture in Figure 3. Larger values are shaded darker. The figure displays the diagonal dominance of the gain matrix. The third column is identically zero due to lack of information about the third actuator.

Despite the third column, it is clear that the gain matrix in Figure 3 has a symmetrical structure. Featherstone and Braatz (1995) summarize several symmetries that are relevant to film-forming processes. Of particular relevance here are centrosymmetric and Toeplitz model structures. A centrosymmetric model has symmetry about the middle of the sheet. The film's response to the first actuator is symmetric to the film's response to the last actuator. Similar relationships exist between the second actuator and the second to last actuator, and so on. The parameters for the centrosymmetric model are calculated by reorganizing the data matrices and then solving the matrix least-squares problem. The reduced problem has only $m/2$ unique actuators, thus the data from actuators $m/2+1$ through m are considered equivalent to data from actuators $m/2$ through 1, respectively. The upper right matrix in Figure 4 shows the result of the least-squares calculation of a centrosymmetric gain matrix using the 3M data set. The shaded pictures are useful for demonstrating structure; however, the parameter values are difficult to discern with accuracy. Therefore, normalized parameters for a typical row (the first row) are presented here:

$$[1.00 \quad 0.73 \quad 0.12 \quad 0.01 \quad -0.26 \quad -0.27 \quad -0.30 \quad -0.33 \quad -0.32 \quad -0.28 \quad -0.31 \quad -0.15].$$

Another type of symmetry arises when all actuators produce shifted versions of the same response. The film's response to the first actuator is the same as its response to the second actuator, although the response is shifted by one lane. A consequence of this shifted film response is that the elements of the gain matrix are constant along the diagonals, and the gain matrix is Toeplitz.

A Toeplitz matrix for a system with m inputs and p outputs has $2m-1$ unique parameters. Enforcing symmetry about the major diagonal leads to a Toeplitz symmetric gain matrix. A Toeplitz symmetric matrix has a total of m unique parameters. In essence each actuator is assumed to be at the center of a sufficiently large sheet. Neither Toeplitz model favorably captures edge effects as well as the centrosymmetric model. Figure 4 shows the least-squares calculation of all four gain matrices discussed in this section. Row-one parameters for the Toeplitz matrix and Toeplitz symmetric matrix are as follows:

$$[1.00 \quad 0.90 \quad 0.37 \quad -0.02 \quad -0.24 \quad -0.33 \quad -0.40 \quad -0.43 \quad -0.36 \quad -0.34 \quad -0.31 \quad -0.30],$$

$$[1.00 \quad 0.69 \quad 0.20 \quad -0.13 \quad -0.32 \quad -0.38 \quad -0.42 \quad -0.43 \quad -0.39 \quad -0.30 \quad -0.32 \quad -0.21].$$

Certainly there is some symmetry associated with this process, although care must be taken not to enforce symmetry that is not present. Figure 5 shows the sum of squares of the residuals from the 36 experiments used to determine the various gain matrices. In the absence of noise and process symmetry, one would expect the residuals to be larger as fewer parameters are used. Consequently, if the process exhibits strong symmetrical behavior, then each model containing the symmetry as a subset of its parameter space would have equivalent residuals. For example, a full-parameter gain matrix with no symmetry contains both centrosymmetric and Toeplitz (regular Toeplitz and Toeplitz symmetric) alternatives as part of its solution set. In the presence of noise, however, the symmetry of the process may be difficult to determine.

In the case of the 3M data, the residuals follow an interesting pattern. The centrosymmetric model with 72 free parameters provides higher residuals than the Toeplitz structure with 23 free parameters. Several interpretations of this result

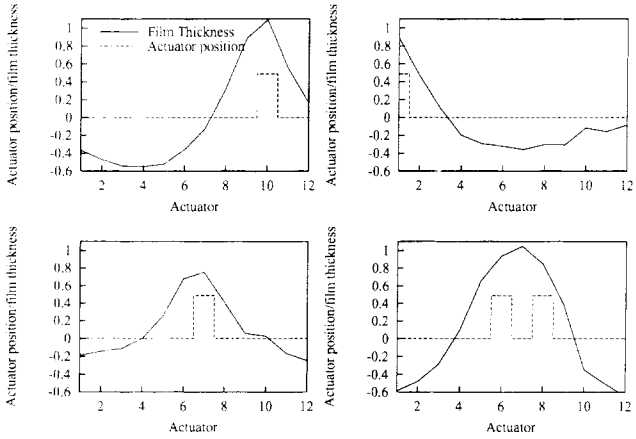

Figure 2. Normalized step test data for the polymer film-forming process.

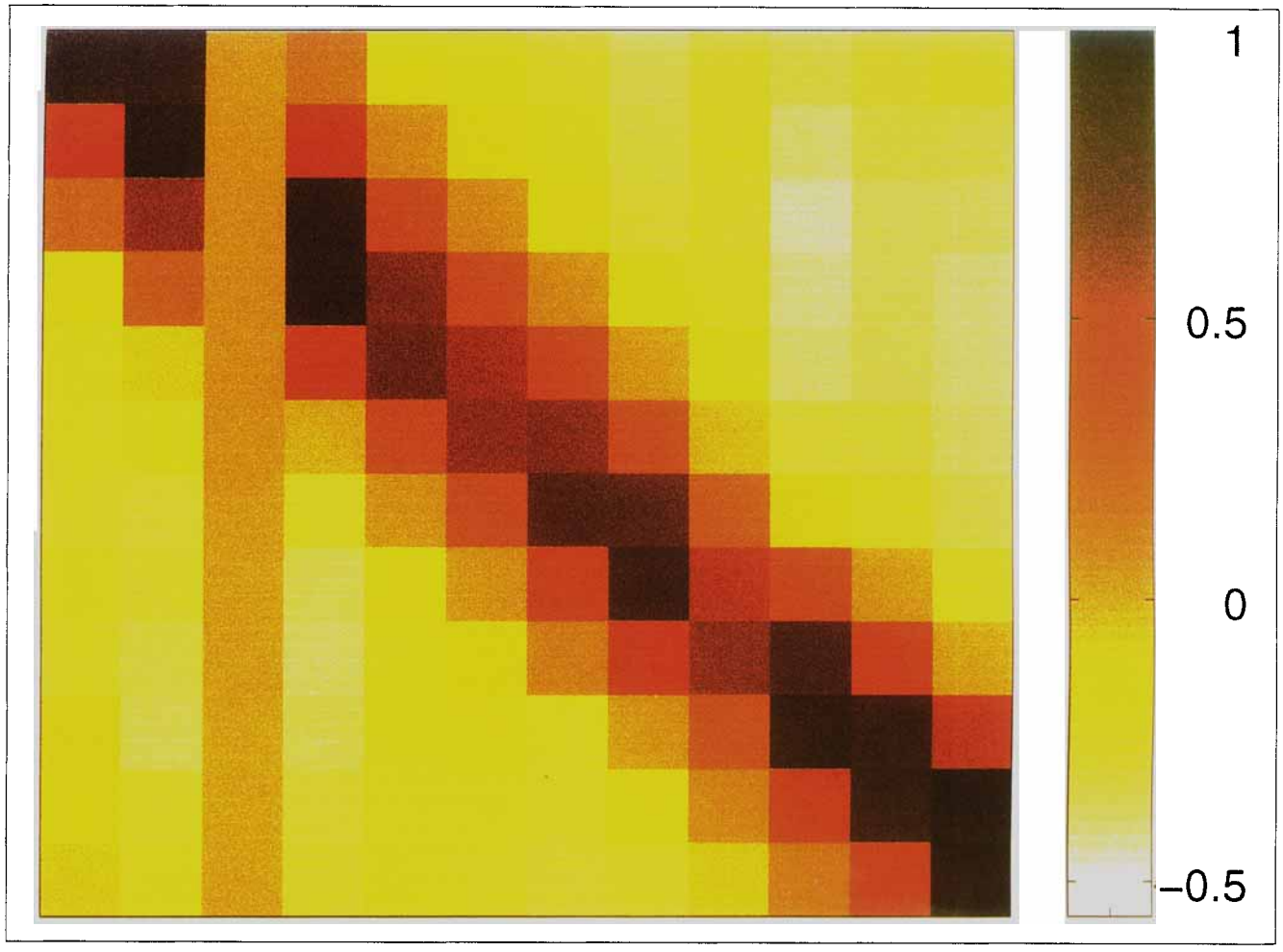

Figure 3. Gain matrix, no symmetry enforced.

Note that the elements corresponding to the third actuator are identically zero.

are possible. First, if the centrosymmetric structure enforces symmetry that is not present, the residuals may be higher. Second, the magnitudes of the residuals might also indicate that the data are noisy and that 36 samples are not enough to obtain quality parameter estimates. If, from previous experiments, it is known that the system exhibits centrosymmetric behavior, then unusually high residuals may indicate a process irregularity such as a die-lip problem or a flow problem.

Estimation

The periodicity of the sensor is readily handled by the Kalman filter (Bergh and MacGregor, 1987; Rawlings and Chien, 1996). Consider the periodic gauge model from Eq. 1, with past inputs included as augmented states (i.e., $x_k = [\tilde{x}_k^T \; u_{k-d}^T \cdots u_{k-1}^T]^T$ in which $\tilde{x}$ is the original state).

$$x_{k+1} = Ax_k + Bu_k + G_\omega \omega_k$$
$$y_k = C_k x_k + \nu_k. \tag{3}$$

The augmented state has dimension $\bar{n} = n + dm$. The state noise, ω_k, is a vector in $\Re^{\bar{n}}$. The measurement or sensor noise, ν_k, is a vector in $\Re^p$. Typically ω_k and ν_k are assumed to be mutually independent, zero-mean white-noise random variables with covariance,

$$E\left\{\begin{bmatrix}\omega_k \\ \nu_k\end{bmatrix}[\omega_k^T \; \nu_k^T]\right\} = \begin{bmatrix}Q_\omega & 0 \\ 0 & R_\nu\end{bmatrix}. \tag{4}$$

In addition, the initial state, x_0, is an independent normally distributed variable with covariance Q_0. It can be shown that with these assumptions the discrete Kalman filter provides the optimal or minimum variance estimate of the state (Jazwinski, 1970). Equation 5 provides the expression for the state estimate, $\hat{x}$. The indexing $\hat{x}_{k|k}$ is read as follows, "the estimate of x at time k given the data up to time k."

$$\hat{x}_{k+1|k} = A\hat{x}_{k|k-1} + Bu_k + L_k(y_k - C_k\hat{x}_{k|k-1}). \tag{5}$$

The filter gain matrix, L_k, can be computed efficiently in terms of the estimate error covariance matrix, P_k,

$$L_k = AP_kC_k^T[C_kP_kC_k^T + R_\nu]^{-1}, \tag{6}$$

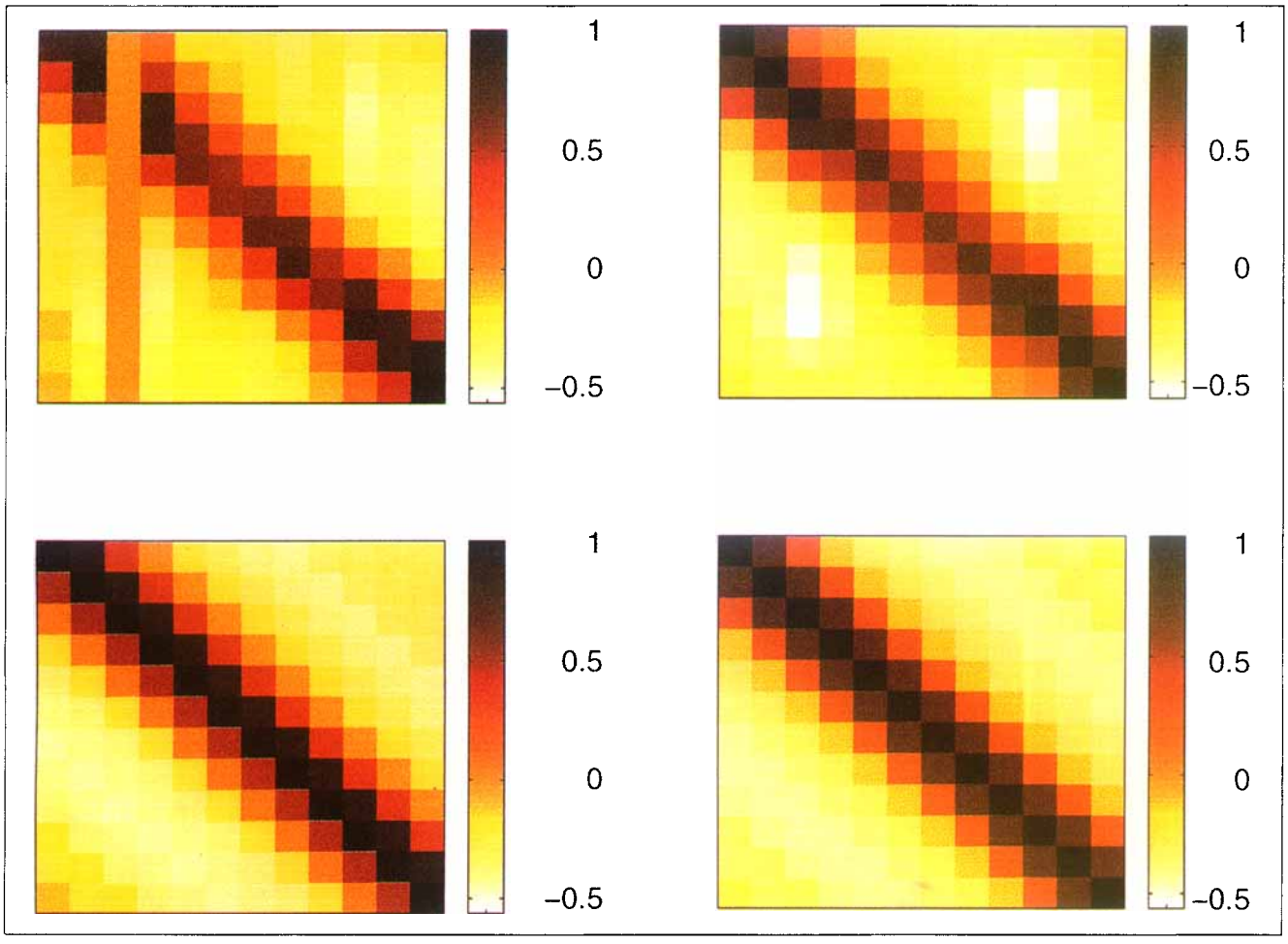

Figure 4. Gain matrices calculated from the data set.

Shown here are the gains calculated with no symmetry enforced (upper left), centrosymmetry enforced (upper right), Toeplitz structure enforced (lower left), and Toeplitz symmetric structure enforced (lower right).

in which P_k can be computed efficiently from the following Riccati iteration,

$$P_{k+1} = AP_kA^T + GQ_\omega G^T - AP_kC_k^T[C_kP_kC_k^T + R_\nu]^{-1}C_kP_kA^T. \quad (7)$$

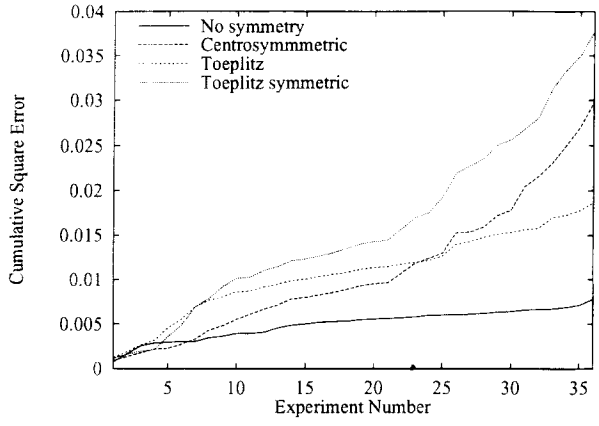

Figure 5. Residuals for the various model types.

Due to the periodic nature of the film and sheet problem induced by the measurement device, a finite number of Kalman filter gains and covariance matrices are computed. The covariance matrices can be used to analyze the potential gain of adding sensors. One such analysis is provided after the following discussion of disturbance models.

Disturbance Models

In order for the controller to remove steady-state offset in the face of modeling errors or nonzero disturbances, a number of integrating disturbance models can be employed. A generic disturbance model is given in Eq. 8:

$$\begin{aligned} x_{k+1} &= Ax_k + Bu_k + G_m z_k + G_\omega \omega_k \\ z_{k+1} &= z_k + \xi_k \\ y_k &= C_k x_k + G_p z_k + \nu_k. \end{aligned} \quad (8)$$

This model employs an integrating disturbance z that can affect either the state or the output; ξ is a zero-mean white-noise random variable with covariance Q_ξ. By considering z

to be part of the state, an augmented state vector can be used to put the system into the general form of Eq. 3. The filter gains for the augmented system can be calculated using Eqs. 6 and 7.

Output disturbance model

The output disturbance model is the most frequently used model in industrial applications (Qin and Badgwell, 1997). An output disturbance model corresponds to $G_m = 0$, $G_p = I$ in Eq. 8. In addition G_p is often chosen such that there is one integrating state in each of the desired outputs. One popular choice of noise characteristics corresponds to a "noise-free" sensor and noisy disturbance state (i.e., $\| Q_\xi \| \gg \| R_\nu \|$, $\| Q_\omega \|$). Calculating the Kalman filter gains and then partitioning the calculating augmented system provides the following equations:

$$\begin{aligned} \hat{x}_{k+1|k} &= A\hat{x}_{k|k-1} + Bu_k + L_x(y_k - C\hat{x}_{k|k-1} - \hat{z}_{k|k-1}) \\ \hat{z}_{k+1|k} &= \hat{z}_{k|k-1} + L_z(y_k - C\hat{x}_{k|k-1} - \hat{z}_{k|k-1}). \end{aligned} \tag{9}$$

For $\| Q_\xi \| \gg \| R_\nu \|$, $\| Q_\omega \|$, $L = [0, I]^T$, and Eq. 9 reduces to

$$\begin{aligned} \hat{x}_{k+1|k} &= A\hat{x}_{k|k-1} + Bu_k \\ \hat{z}_{k+1|k} &= y_k - C\hat{x}_{k|k-1}. \end{aligned} \tag{10}$$

Equation 10 is the QDMC (García and Morshedi, 1986) estimator, where at each sample time z is the difference between the measurement and the model estimate. This value is predicted to be constant in the future for the control calculations.

Other choices of G_p and G_m provide other useful disturbance models. The input disturbance model with $G_p = 0$ and $G_m = B$ is a logical choice if disturbances come from upstream sources, although for the highly correlated film process, the input disturbance model has undesirably slow disturbance rejection (Campbell, 1997). Another disturbance model relevant to gauge control is the measured input disturbance model. This model requires additional measurements, however, and is therefore presented next as a separate model.

Measured input disturbance model

The measured input disturbance model requires additional measurements that may not be available to the controller. The actual measurement required is a measurement of the *input*. These measurements can prove useful in the case of large time-delay systems, or systems subject to frequent actuator failures.

The measured input disturbance model is shown below with z as the estimate of the input bias and $y^m \in \Re^m$:

$$\begin{aligned} x_{k+1} &= Ax_k + B(u_k + z_k) + G_\omega \omega_k \\ z_{k+1} &= z_k + \xi_k \\ y_k &= C_k x_k + \nu_k \\ y_k^m &= (u_k + z_k) + \eta_k. \end{aligned} \tag{11}$$

As with the general disturbance model, the state can be augmented with z in order to calculate the filter gains. In this case, augmentation produces a D matrix that, similar to the B matrix, can be ignored during the calculation of the Kalman filter gains.

Detectability of Disturbance Models

In this section detectability conditions for the disturbance models presented in the previous section are discussed. Detectability of the combined process and disturbance models implies observability of the disturbance states. In other words, the data are informative enough to determine uniquely the values of the states and disturbances given the model.

Theorem 1 (Detectability of the Disturbance Augmented System). The periodic disturbance model presented in Eq. 8 is detectable if and only if (A, C_k) is detectable and

$$\begin{bmatrix} I_n - \mathfrak{A} & \mathfrak{G}_m \\ \mathfrak{C} & \mathfrak{G}_c \end{bmatrix} \tag{12}$$

is full column rank. $\mathfrak{A}$, $\mathfrak{C}$, $\mathfrak{G}_m$, and $\mathfrak{G}_c$ are defined as follows.

$$\mathfrak{A} = A^q \qquad \mathfrak{G}_m = [A^{q-1}G_m \quad A^{q-2}G_m \cdots G_m] \tag{13}$$

$$\mathfrak{C} = \begin{bmatrix} C_0 \\ C_1 A \\ \vdots \\ C_{q-1}A^{q-1} \end{bmatrix}$$

$$\mathfrak{G}_c = \begin{bmatrix} G_p & 0 & 0 & \cdots & 0 \\ C_1 G_m & G_p & 0 & \cdots & 0 \\ C_2 A G_m & C_2 G_m & G_p & \cdots & 0 \\ \vdots & \vdots & \ddots & \ddots & \vdots \\ C_{q-1}A^{q-2}G_m & C_{q-1}A^{q-3}G_m & \cdots & C_{q-1}G_m & G_p \end{bmatrix}. \tag{14}$$

Remark 1. Theorem 1 can be proved by constructing a lifted analog to the periodic system and utilizing the Hautus Detectability Lemma. Lifted systems, which are time-invariant representations of periodic systems, are presented in the context of coating-, sheet-, and film-forming processes by Goodwin and coworkers (1994), Tyler and Morari (1995), and Feuer and Goodwin (1996). Lifted disturbance models corresponding to the disturbance models in Eqs. 8 and 11 can be found in Campbell (1997). Since the periodic system and the lifted system are equivalent systems, the Hautus condition applied to the lifted system provides a straightforward way to prove Theorem 1. The details of the proof and construction of the lifted systems are omitted for brevity. The complete proof is provided in Campbell (1997).

Theorem 1 provides a starting point for the analysis of several disturbance models. One immediate consequence of Eq. 12 is that no disturbance model can have more disturbance

states than the number of outputs and retain detectability. In addition to the requirement that there are less disturbance states than outputs, care must be taken to ensure that the remaining disturbance states are distinguishable from the system's own integrators.

Theorem 2 (Detectability of the Measured Disturbance Augmented System). The periodic disturbance model in Eq. 11 is detectable if and only if (A, C_k) is detectable.

Remark 2. Theorem 2 also can be proved by constructing a lifted analog to the periodic system and utilizing the Hautus Detectability Lemma. Because the model specifies one disturbance state for each input and each disturbance is added to only one input, no additional rank condition is necessary. See Campbell (1997) for the proof.

Covariance analysis example

The covariances of the estimates can be used to evaluate quantitatively the improvement gained by employing additional sensors. Tyler and Morari (1995) provide a comparison of estimates from scanning and stationary sensors. In this work, the covariance of the original model state estimates is not important because the system is assumed to have instantaneous dynamics. In other words, the predicted state does not depend on the current state, and thus a quality estimate of the current state is unnecessary. The use of a disturbance model, however, incorporates new disturbance states for which quality estimates are needed.

In the following example a process with 60 lanes is analyzed. An output disturbance model is used with three different G_p matrices to account for various levels of correlation between lanes. The covariance matrix provides a measure of the quality of the estimate. A hyperellipsoid of constant probability in the estimate space can be constructed using the covariance matrix. See Bard (1974) for details on the probabilistic interpretation of the covariance matrix. For this study, it is sufficient to consider the square root of the diagonal elements of the covariance matrix as a measure of the quality of the state estimate. Since there are 60 estimates at each sample time and several sample times in each scanning sensor period, an average of all estimates throughout the period is used to compare the simulation results.

With each additional scanner that is added, the scanning pattern is altered. The pattern is chosen such that the scanners are a fixed distance apart at all times and each scanner measures a unique section of the sheet. For example, three scanners would start in lanes 1, 21, and 41 and travel to 20, 40, and 60, respectively, before returning to their original positions. This pattern avoids redundant measurements and minimizes the period of the scanners.

Consider first the case in which $G_p = I$. As the number of sensors increases, the average disturbance state covariance decreases. The result is shown in Figure 6. $G_p = I$ is a physically unlikely disturbance model because it implies that disturbances that affect a given lane do not affect the neighboring lanes. A more correlated model with a banded G_p matrix is used next. The band provides a tent-shaped disturbance that reaches four lanes on either side of a given lane. Finally, a banded G_p matrix affecting nine lanes on either side is used.

Figure 6 shows the results of these simulations. Two conclusions can be drawn from the results. First, the effect of

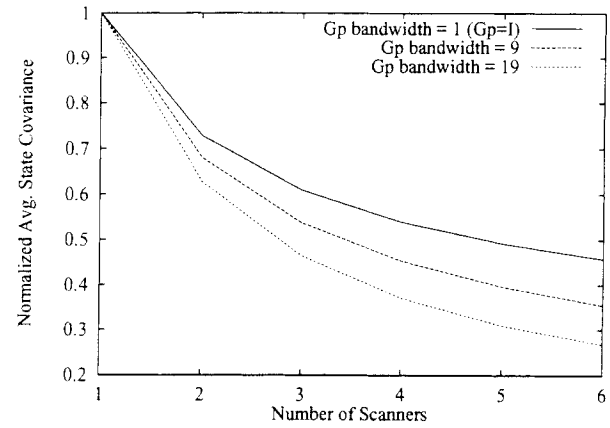

Figure 6. Average disturbance state covariance vs. number of scanners for various levels of correlation in the disturbance model.

adding a sensor to a single-sensor system is much more significant than adding a sensor to a system with several sensors. The second conclusion concerns the correlation of the disturbances. The more correlated the disturbances, the more benefit attained from adding sensors.

Regulation

The regulator proposed for this work is a constrained infinite-horizon regulator. The full infinite-horizon control problem is solved by using an input parameterization. Several researchers have exploited the idea of this input parameterization (Sznaier and Damborg, 1987; Chmielewski and Manousiouthakis, 1996; Scokaert and Rawlings, 1996b; Scokaert and Rawlings, 1997). Since the A matrix is zero in the film-process model, the infinite-horizon control problem reduces to the regulator problem proposed by Muske and Rawlings (1993). The full infinite-horizon problem is shown in Eq. 15.

Infinite Horizon Control: Constrained.

$$\min_{\pi} \Phi_N(x_0, \pi)$$

subject to:

$$\Phi_N(x_0, \pi) = \sum_{j=0}^{\infty} z_j^T Q z_j + v_j^T R v_j \quad Q \geq 0, \quad R > 0$$

$$z_{j+1} = Az_j + Bv_j$$

$$z_0 = x_0$$

$$Hz_j \leq h \quad j = 0, 1, \ldots, N-1$$

$$Dv_j \leq d \quad j = 0, 1, \ldots, N-1$$

$$v_j = -Kz_j \quad j = N, \ldots, \infty. \tag{15}$$

Figure 7 illustrates the contributions to the objective function. While an infinite number of inputs are considered, only a finite number are decision variables in the quadratic pro-

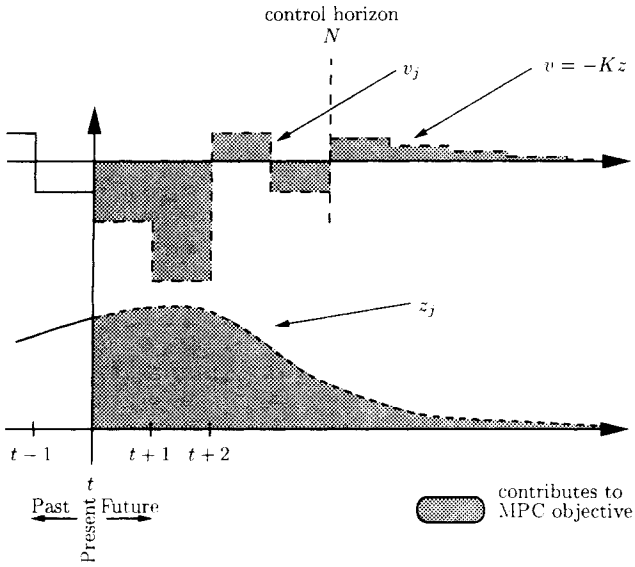

Figure 7. Infinite-horizon control with $v_k = -Kz_k$ for $k \geq N$.

gram ($\pi = \{v_0, v_1, \ldots, v_{N-1}\}$). A finite QP is formulated by setting $v_k = -Kz_k$ for $k \geq N$, where K is the solution to the unconstrained linear quadratic regulator problem. The infinite sum in the objective function given in Eq. 15 can be evaluated as follows:

$$\Phi_N(x_0, \pi) = \sum_{j=0}^{N-1} \left(z_j^T Q z_j + v_j^T R v_j \right) + z_N^T \tilde{Q} z_N, \qquad (16)$$

in which $\tilde{Q}$ can be calculated from the standard Riccati equation measuring optimal cost to go from state z_N.

Special consideration is given to the constraints on the infinite horizon since the optimization only ensures that the constraints are satisfied over the first N time steps (Scokaert and Rawlings, 1996a). The quadratic program is solved and if there are constraint violations, then N is increased and the problem is resolved. There exists a finite N that enforces the constraints over the infinite horizon. See Scokaert and Rawlings (1996b) for further details of the implementation and Gilbert and Tan (1991) for further discussion of the general idea of output-admissible sets.

For large-scale sheet- and film-forming processes, the control problem approaches sizes that are prohibitive for real-time control. The quadratic program resulting from the control problem presented in Eq. 15 has a special structure that can be exploited using structured interior point methods. See Rao et al. (1997a,b) for details on significantly increasing the speed of solution for the constrained infinite-horizon regulation problem.

Target Tracking

The previous section used zero targets for the regulation problem. It was assumed that a steady-state target was available and then deviation variables were used to recast the problem in the form presented in Eq. 15. This section discusses the determination of steady-state input and state targets from set points u_{sp} and y_{sp} and input and output constraints.

Since targets are not always needed for all outputs, an alternative measurement matrix ($\acute{C}$) can be specified. Full row rank of $\acute{C}$ is required because redundant set points or void set points (zero rows) are unimportant cases. Additional system requirements include (A, $\acute{C}$) detectable and (A, B) stabilizable. Calculating targets for undetectable or unstabilizable systems is possible in certain circumstances, but makes little sense from a practical point of view. The steady-state targets are denoted x_t and u_t. The steady-state system equations are given by

$$\begin{aligned} x_t &= Ax_t + Bu_t \\ y_t &= \acute{C}x_t. \end{aligned} \qquad (17)$$

Muske and Rawlings (1993) determine the targets by solving up to two quadratic programs. The first quadratic program solves Eq. 17 exactly while setting $y_t = y_{sp}$ and penalizing any degrees of freedom in the input. Because this quadratic program frequently has an empty feasible set (e.g., there is no x_t such that $\acute{C}x_t = y_{sp}$), a second quadratic program is solved in which the least-squares solution from the output set point is calculated. As an alternative to the two-stage target-tracking problem a single exact soft-constraint problem is proposed here.

Exact soft-constraint target determination

It is desirable to solve only one target calculation that provides the same solution that the multistep target calculation provides. One calculation can be done with exact soft constraints. The main idea behind soft constraints is that constraints are met when feasible. See Fletcher (1987) for more details on exact penalty methods on which soft constraints are based. For this study, it is sufficient to relax the equality constraint $y_{sp} = \acute{C}x_t$ by redefining the constraint in terms of a slack variable ϵ:

$$\epsilon \geq y_{sp} - \acute{C}x_t \qquad (18)$$

$$\epsilon \geq -\left(y_{sp} - \acute{C}x_t\right) \qquad (19)$$

$$\epsilon \geq 0. \qquad (20)$$

In addition to penalizing a quadratic measure of ϵ, a linear penalty, $S^T\epsilon$, is used, in which the weighting vector S has strictly nonnegative values. Appropriate choice of S ensures the exact-penalty property. De Oliveira and Biegler (1994) provide further discussion of exact penalties in predictive control. The target-tracking problem is presented in Eq. 21.

Exact Soft Constraint Target Tracking.

$$\min_{[u_t, x_t, \epsilon]^T} \Phi(\epsilon, u_t, u_{sp})$$

subject to:

$$\Phi(\epsilon, u_t, u_{sp}) = \epsilon^T Q_s \epsilon + (u_t - u_{sp})^T R_s (u_t - u_{sp}) + S_s^T \epsilon$$

$$Q_s, R_s, S_s > 0$$

$$x_t = Ax_t + Bu_t$$

$$y_{sp} - \acute{C}x_t \le \epsilon$$

$$-\left(y_{sp} - \acute{C}x_t\right) \le \epsilon$$

$$Hx_t \le h$$

$$Du_t \le d. \qquad (21)$$

It is of interest to guarantee that the solution to Eq. 21 is unique to ensure the steady-state target is well defined. The following theorem is due to Rao (personal communication, 1997) and is proved in the Appendix.

Theorem 3 (Exact Soft-Constraint Target Tracking). The feasible quadratic program in Eq. 21 has a unique solution for $(A, \acute{C})$ detectable.

The feasible quadratic program in Eq. 21 with $\epsilon = 0$ solves Eq. 17 exactly; thus, the exact target-tracking solution is obtained.

Simulation: Measured Inputs

The data set used to produce the gain matrix from the 3M data is lacking information regarding the third actuator. Symmetry can be exploited to overcome these missing data during model identification, but the question remains as to how the controller performs when faced with actuator failure and actuator bias. In this section we examine how actuator bias and actuator failure can be handled. The comparison is between the output disturbance model and a measured input model.

The process has 12 measured lanes and 12 actuators. The model assumes fast actuator dynamics ($A = 0$) and a time delay equal to the number of lanes. The centrosymmetric gain matrix from Figure 4 is used in the model. All inputs have upper and lower constraints of 1, -1, respectively.

In the first simulation, the actuator in lane six has a bias of 0.5 (it consistently opens too far). The output disturbance model is used to compensate for the bias. The entire state of the film is shown in Figure 8. Recall that the sensor only "sees" one lane at a time. By the time the disturbance is seen by the sensor (chosen to be time = 14), the sensor is in lane

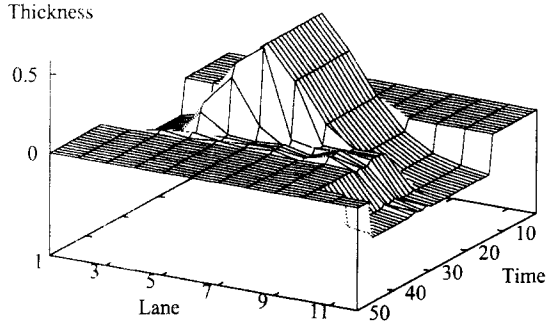

Figure 8. Biased actuator simulation using scanning sensor, optimal output disturbance filter, and model-predictive controller.

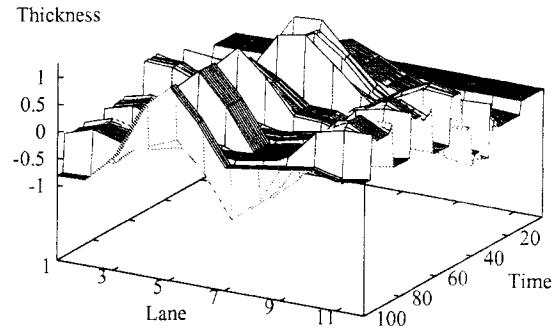

Figure 9. Disabled-actuator simulation using scanning sensor, optimal output disturbance filter, and model-predictive controller.

10 and moving toward lane one. After the sensor passes through all lanes (past lane 10 again to lane 12 at time = 34) it can properly reconstruct the state. After 12 more time steps, the disturbance is adequately removed.

Figure 9 displays how the output disturbance model handles the situation in which the sixth actuator is disabled and stuck at 0.5. The controller attempts to use the sixth actuator even though it does not respond. The estimates of the error converge to a periodic set of values that provide undesirable performance. Figure 10 shows the mean square error of the gauge profile vs. time. Often, a disturbance model designed for one type of disturbance can provide adequate performance in the face of other types of disturbances. Clearly, that is not the case here, and a better model is required to solve this problem. Measurement of actuator position can solve this problem efficiently.

The next simulation demonstrates the use of a measured input disturbance model. The actuator positions are provided to the estimator at each time step; Figure 11 shows the film's response. The disturbance state in lane six takes only two time steps to wind up and correctly identify the bias. If the estimator were used with an unconstrained regulator, the regulator would continue to send larger input values to counter the bias, thus making the bias larger. The estimator

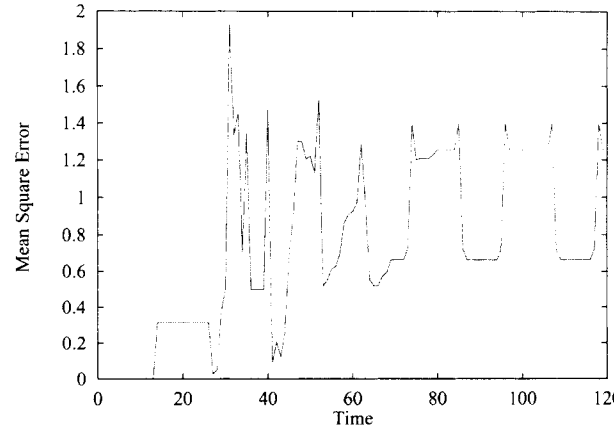

Figure 10. Mean square error of film thickness corresponding to disabled-actuator simulation in Figure 9.

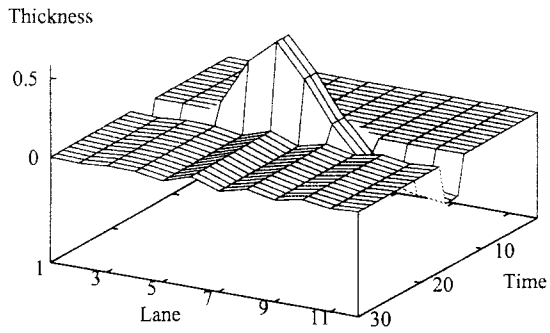

Figure 11. Disabled-actuator simulation using scanning sensor, optimal measured input disturbance filter, and model-predictive controller.

used with the constrained regulator, however, winds up the bias estimate and adjusts the remaining actuators to flatten the film. Note also that this simulation is using many more data (12 input measurements and 12 output measurements) to determine the state of the system than the previous two simulations. As expected, this model also works well for the case of actuators with bias.

Conclusions

A linear model with fast dynamics, a large time delay, and a periodic measurement matrix was employed for sheet- and film-forming processes. The model parameters were identified from process data, and process symmetry was used to improve parameter estimates. The symmetry allowed identification of gain-matrix parameters from an incomplete data set. Care must be taken not to enforce symmetry in the model that is not present in the process. In this work, the centrosymmetric model provided slightly higher residuals than the Toeplitz structure model. More data are needed to determine if this result is related to noisy data or if the gain matrix is best described by a Toeplitz structure.

The periodic Kalman filter was employed as a method for determining optimal state estimates. The Kalman filter is useful because disturbance models are easily incorporated into the formulation. A disturbance model is used because integrating disturbance states used in conjunction with model-predictive controllers provide offset-free control. A general disturbance model was presented from which the output disturbance model was constructed. A measured input disturbance model was also presented. This model requires additional system measurements, but is able to handle actuator bias and actuator failure. Detectability conditions for both the general disturbance model and the measured input disturbance model were presented.

Simulations show improvement of the estimates with increasing number of sensors. Although scanning sensors are expensive, a 30% reduction in the covariance of the estimates is achieved by adding a second sensor. Adding additional sensors provides less dramatic reductions in the estimates. The effect of adding sensors is greater for correlated models in which the disturbances are assumed to affect several neighboring lanes.

An infinite-horizon regulator was used for control. Target determination was addressed with an exact soft-constraint formulation as a method of meeting set points when feasible. The steady-state target solution was shown to be unique for detectable systems and positive definite penalty matrices.

An optimal output disturbance estimator was used in simulation with both actuator bias and actuator failure. This estimator rejected the actuator bias disturbance, but needed time to scan the entire film. The estimator was unable to provide adequate performance when an actuator failed. By measuring the inputs at each time step, a measured input disturbance estimator was able to remove both types of actuator problems independent of the process time delay. This second estimator requires additional measurements. When actuator bias and failure is prevalent, however, the cost of installing these sensors may be justified by the improved performance.

Acknowledgments

Financial support from 3M, DuPont, Weyerhaeuser, and the National Science Foundation under Grant CTS-9311420 is gratefully acknowledged.

Literature Cited

Bard, Y., *Nonlinear Parameter Estimation*, Academic Press, New York (1974).

Bergh, L. G., and J. F. MacGregor, "Spatial Control of Sheet and Film Forming Processes," *Can. J. Chem. Eng.*, **65**, 148 (1987).

Boyle, T. J., "Control of Cross-Direction Variations in Web Forming Machines," *Can. J. Chem. Eng.*, **55**, 457 (1977).

Campbell, J. C., *Modelling, Estimation, and Control of Sheet and Film Forming Processes*, PhD Thesis, Univ. of Wisconsin-Madison (1997).

Campbell, J. C., and J. B. Rawlings, "Estimation and Control of Sheet and Film Forming Processes," *Control Problems in Industry*, I. Lasiecka and B. Morton, eds., SIAM, Birkhäuser, Boston, p. 43 (1995).

Chmielewski, D., and V. Manousiouthakis, "On Constrained Infinite-Time Linear Quadratic Optimal Control," *Syst. Contr. Lett.*, **29**, 121 (1996).

Corscadden, K. W., and S. R. Duncan, "The Use of Basis Function Expansions to Analyse the Robustness of Cross-Directional Control Systems," *Proc. Amer. Control Conf.*, Albuquerque, NM, p. 1478 (1997).

Dave, P., D. A. Willig, G. K. Kudva, J. F. Pekny, and F. J. Doyle, "LP Methods in MPC of Large-Scale Systems: Application to Paper-Machine CD Control," *AIChE J.*, **43**, 1016 (1997).

de Oliveira, N. M. C., and L. T. Biegler, "Constraint Handling and Stability Properties of Model-Predictive Control," *AIChE J.*, **40**, 1138 (1994).

Dumont, G. A., "Application of Advanced Control Methods in the Pulp and Paper Industry—A Survey," *Automatica*, **22**, 143 (1986).

Dumont, G. A., "Challenges in Control of Web Processes," *IFAC Adchem: Int. Symp. on Advanced Control of Chemical Processes*, Banff, Alberta, Canada (1997).

Featherstone, A. P., and R. D. Braatz, "Control Relevant Identification of Sheet and Film Processes," *Proc. American Control Conf.*, Seattle, WA, p. 2692 (1995).

Featherstone, A. P., and R. D. Braatz, "Control-Oriented Modeling of Sheet and Film Processes," *AIChE J.*, **43**, 1989 (1997).

Feuer, A., and G. C. Goodwin, *Sampling in Digital Signal Processing and Control*, Birkhauser, Boston (1996).

Fletcher, R., *Practical Methods of Optimization*, Wiley, New York (1987).

García, C. E., and A. M. Morshedi, "Quadratic Programming Solution of Dynamic Matrix Control (QDMC)," *Chem. Eng. Commun.*, **46**, 73 (1986).

Gilbert, E. G., and K. T. Tan, "Linear Systems with State and Control Constraints: The Theory and Application of Maximal Output Admissible Sets," *IEEE Trans. Automat. Contr.*, **AC-36**, 1008 (1991).

Golub, G. H., and C. F. V. Loan, *Matrix Computations*, Johns Hopkins Univ. Press, Baltimore, MD (1989).

Goodwin, G. C., S. J. Lee, A. Carlton, and G. Wallace, "Application of Kalman Filtering to Zinc Coating Mass Estimation," *Proc. IEEE Conf. on Control Applications*, Glasgow, Scotland (1994).
Jazwinski, A. H., *Stochastic Processes and Filtering Theory*, Academic Press, New York (1970).
Kristinsson, K., and G. A. Dumont, "Cross-Directional Control of Paper Machines Using Gram Polynomials," *Automatica*, **32**, 533 (1996).
Muske, K. R., and J. B. Rawlings, "Model Predictive Control with Linear Models," *AIChE J.*, **39**, 262 (1993).
Qin, S. J., and T. A. Badgwell, "An Overview of Industrial Model Predictive Control Technology," *Chemical Process Control—V*, J. C. Kantor, C. E. García, and B. Carnahan, eds., CACHE, AIChE, p. 232 (1997).
Rao, C. V., J. C. Campbell, J. B. Rawlings, and S. J. Wright, "Efficient Implementation of Model Predictive Control for Sheet and Film Forming Processes," *Proc. Amer. Control Conf.*, Albuquerque, NM, p. 2940 (1997a).
Rao, C. V., S. J. Wright, and J. B. Rawlings, "On the Application of Interior Point Methods to Model Predictive Control," Preprint, Mathematics and Computer Science Div., Argonne National Laboratory, Argonne, IL (1997b).
Rawlings, J. B., and I.-L. Chien, "Gage Control of Film and Sheet-Forming Processes," *AIChE J.*, **42**, 753 (1996).
Rigopoulos, A., Y. Arkun, and F. Kayihan, "Identification of Full Profile Disturbance Models for Sheet Forming Processes," *AIChE J.*, **43**, 727 (1997).
Scokaert, P. O., and J. B. Rawlings, "Infinite Constraint Horizons in MPC," AIChE Meeting, Chicago (1996a).
Scokaert, P. O., and J. B. Rawlings, "Constrained Linear Quadratic Regulation," *IEEE Trans. Automat. Contr.* (1998).
Scokaert, P. O. M., and J. B. Rawlings, "Infinite Horizon Linear Quadratic Control with Constraints," *Proc. IFAC World Cong.*, San Francisco (1996b).
Sontag, E. D., *Mathematical Control Theory*, Springer-Verlag, New York (1990).
Sznaier, M., and M. J. Damborg, "Suboptimal Control of Linear Systems with State and Control Inequality Constraints," *Proc. Conf. on Decision and Control*, p. 761 (1987).
Tyler, M. L., and M. Morari, "Estimation of Cross Directional Properties: Scanning versus Stationary Sensors," *AIChE J.*, **41**, 846 (1995).
VanAntwerp, J. G., R. D. Braatz, and N. V. Sahinidis, "Globally Optimal Robust Control of Large Scale Sheet and Film Processes," *Proc. Amer. Control Conf.*, Albuquerque, NM, p. 1473 (1997).
Wilhelm, R. G., Jr., and M. Fjeld, "Control Algorithms for Cross Directional Control: The State of the Art," *Proc. IFAC/IMEKO Conf. on Instrumentation in the Paper, Rubber, Plastic and Polymerization Industries*, Antwerp, The Netherlands (1983).
Zhang, J., "Model Predictive Control of Sheet and Film Forming Processes," MS Thesis, Univ. of Wisconsin-Madison (1997).

Appendix

Theorem 3 (Exact Soft-Constraint Target Tracking). The feasible quadratic program in Eq. 21 has a unique solution for $(A, \acute{C})$ detectable.

Proof. It is sufficient to have a strictly convex quadratic program (Fletcher, 1987). Strictly convex requires positive definite Hessian and affine constraints.

Consider first the case where A has no eigenvalues at 1. Since $(I - A)$ is invertible, the equality constraint can be used to eliminate x_t from the problem:

$$x_t = (I - A)^{-1} B u_t. \tag{A1}$$

Since R is positive definite and the constraints are affine, the strictly convex quadratic problem has a unique global solution.

Consider now the case where A has at least one eigenvalue at 1. The Hautus Detectability Lemma (Sontag, 1990) implies the following rank condition, rank $(\mathcal{H}) = N$

$$\mathcal{H} = \begin{bmatrix} \lambda I - A \\ \acute{C} \end{bmatrix} \tag{A2}$$

for all $\lambda \in \mathbb{C}$ with magnitude greater than or equal to 1. It is sufficient to consider only the Hautus matrix, $\mathcal{H}$, with $\lambda = 1$. Due to detectability, $\mathcal{H}$ has full column rank. It then follows that x_t is uniquely determined from the following equation

$$\mathcal{H} x_t = \begin{bmatrix} B u_t \\ y_{sp} \pm (\epsilon - s) \end{bmatrix}, \tag{A3}$$

where s is a positive slack for the inequality constraints. Partitioning the columns of the pseudoinverse of $\mathcal{H}$ allows x_t to be eliminated from the constraint equations. Since the remaining constraints represent an affine relationship between u_t and $(\epsilon - s)$, it follows that Eq. 21 is strictly convex. Since the quadratic program is strictly convex for both situations, the solution is unique as claimed.

Manuscript received June 17, 1997, and revision received May 18, 1998.